Electronic Supplementary Material (ESI) for Journal of Materials Chemistry C.
This journal is © The Royal Society of Chemistry 2022

Supporting Information

Nan Wang[1#], Rui Sun[1#], Wen Xu[2]*, *Xue Bai [1], Junhua Hu[3], Siyu Lu[4],* Donglei Zhou[1]*, Hongwei Song[1]*

[1] State Key Laboratory on Integrated Optoelectronics, College of Electronic Science and Engineering, Jilin University, Changchun, 130012, China.

[2]Key Laboratory of New Energy and Rare Earth Resource Utilization of State Ethnic Affairs Commission, Dalian Minzu University, Dalian, 116600, China.

[3]State Centre for International Cooperation on Designer Low-Carbon & Environmental Materials, School of Materials Science and Engineering, Zhengzhou University, Zhengzhou 450001, China.

[4] College of Chemistry, Zhengzhou University, Zhengzhou, 450001, China.

[*]E-mail: Prof. Wen Xu (xuwen@dlnu.edu.cn), Prof. Donglei Zhou (zhoudl@jlu.edu.cn), Prof. Hongwei Song (songhw@jlu.edu.cn)

Experimental

1. Chemicals

1-octadecene (ODE, 90%), oleic acid (OA, 90%), oleylamine (OAm，70%)，cyclohexane，lead chloride ($PbCl_2$), manganese chloride ($MnCl_2$), antimony trichloride ($SbCl_3$), and toluene, ethyl acetate. All chemicals were directly used without further purification.

2. Preparation of Cs-oleate

0.407g of Cs_2CO_3, 10 ml of ODE, and 1.25 ml OA were loaded into a 20 ml glass bottle. The mixture was heated for 1h at 130 °C until Cs_2CO_3 was completely dissolved to form a clear solution.

3. Synthesis of the Mn^{2+} doped or Mn^{2+} and Sb^{3+} co-doped $CsPbCl_3$ NCs. The Mn^{2+} doped or Mn^{2+} and Sb^{3+} co-doped $CsPbCl_3$ NCs were synthesized by hot injection method. In a typical synthesis, 0.375 mmol of $PbCl_2$, $MnCl_2$ (and $SbCl_3$), ODE (10 ml), OA (1ml), and OAm (1ml) were loaded into a 100 ml three-necked flask and heated at 130°C for 1h under N_2 atmosphere. Then the reaction temperature of the mixture was increased to 180°C and 1 ml of the Cs-oleate precursor was rapidly injected. After that, the mixture solution was kept at 180°C for 30s. Then, the reaction solution was cooled in cold water. The Mn^{2+}, Sb^{3+} co-doped $CsPbCl_3$ NCs were obtained by regulating the molar feed ratio of $MnCl_2/SbCl_3$.

Characterization：TEM images were collected by Hitachi H-800 at 200KV. HRTEM and mapping were measured by JEM-2100F at 200KV. Absorption spectra were collected with UV/vis- spectrophotometer (Shimadzu UV-1800). Photoluminescence spectra were recorded on a Shimadzu RF-6000 spectrofluorometer. X-Ray Diffraction (XRD) patterns were measured by using a Bruker D8 diffractometer with Cu Kα radiation. Time-resolved emission decay curves were measured using a PLS980 time correlated single-photon counting (TCSPC) system. Low-temperature fluorescence spectroscopy was acquired using a tuneable optical parameter oscillator (OPO) as the excitation source and a visible photomultiplier (350–850 nm) combined with a double-grating monochromator for spectral collection. X-ray photoelectron spectroscopy (XPS) was collected by Kratos Axis UltraDLD. Absolute emission QY values were measured at room temperature using a commercial integrating sphere installed in FLS980 spectrometer from Edinburgh Instruments. Calibration of the photoluminescence QY value was performed using the standard sample YAG:Ce^{3+} (BM302D, Jiangsu Bree Optronics Co., Ltd, peaking at 551 nm).

Calculation method

First-principle calculations were performed by the density functional theory (DFT) using the Vienna Ab-initio Simulation Package (VASP) package.[1] The generalized gradient approximation (GGA) with the Perdew−Burke−Ernzerhof (PBE) functional were used to describe the electronic exchange and correlation effects.[2] Uniform G-

centered k-points meshes with a resolution of 2π*0.04 Å-1 and Methfessel-Paxton electronic smearing were adopted for the integration in the Brillouin zone for geometric optimization. The simulation was run with a cutoff energy of 500 eV throughout the computations. These settings ensure convergence of the total energies to within 1 meV per atom. Structure relaxation proceeded until all forces on atoms were less than 1 meV Å-1 and the total stress tensor was within 0.01 GPa of the target value. For the Mn^{2+}- and Sb^{3+}-doped $CsPbCl_3$ structure, $CsPbCl_3$ with tetragonal structure (space group: P4mm) was selected, and then we build a 2*2*2 supercell structure based on $CsPbCl_3$ unit cell, in which one Pb atom was replaced by Mn and the other Pb atom was replaced by Sb.

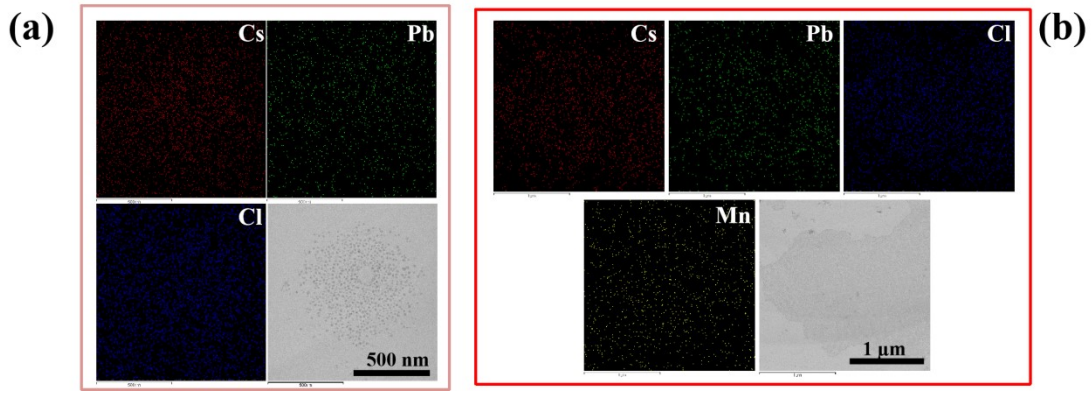

Fig. S1. EDS mapping images for (a) $CsPbCl_3$, (b) $CsPbCl_3$:Mn^{2+}. It can be seen that the elements in each material are evenly distributed.

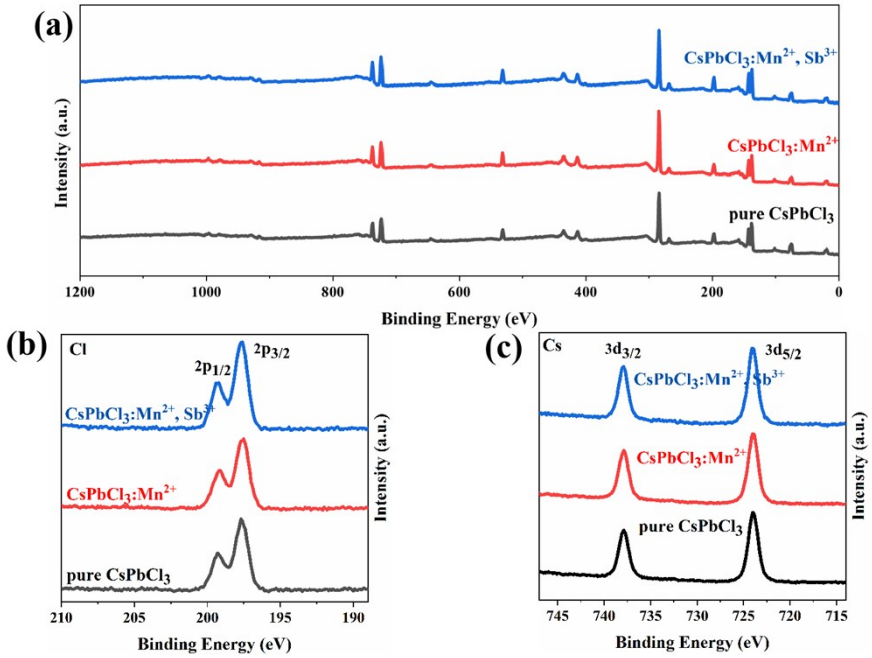

Fig. S2. (a) XPS total patterns, high-resolution XPS analysis of (b) Cl 2p and (c) Cs 3d for pure $CsPbCl_3$, $CsPbCl_3$:Mn^{2+} and $CsPbCl_3$:Mn^{2+}, Sb^{3+} respectively.

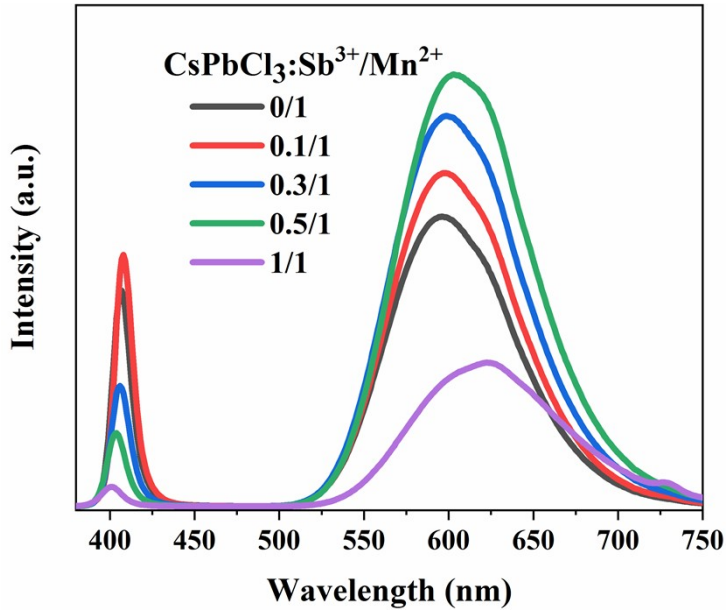

Fig. S3. Steady-state PL spectra for $CsPbCl_3$ NCs with varied the moral ratio of Sb^{3+}/Mn^{2+} upon the excitation of 365 nm source.

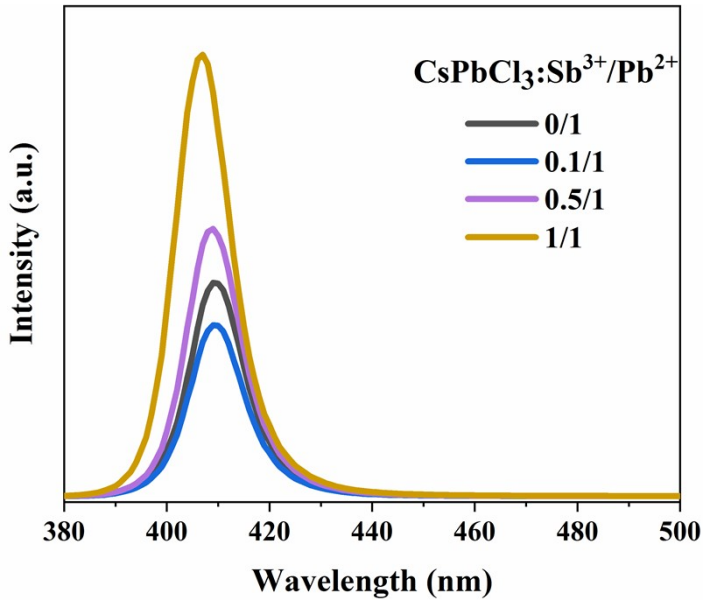

Fig. S4. PL spectra of $CsPbCl_3$ NCs with only Sb^{3+} doping and changing the Sb^{3+}/Pb^{2+} molar ratio under excitation at 365 nm .

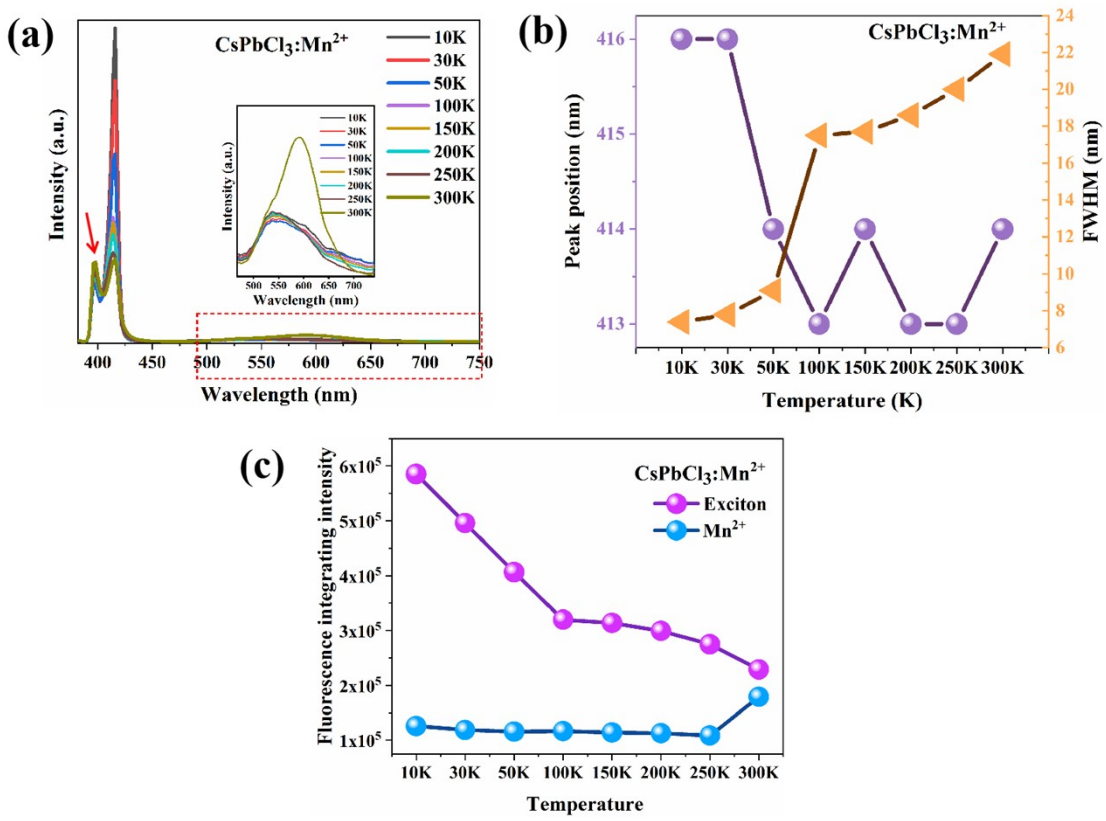

Fig. S5. (a) Temperature-dependent steady-state spectra (inset: enlarged image inside the dashed box) and (b) corresponding peak position and FWHM curves for $CsPbCl_3:Mn^{2+}$ sample. (c) The plot of integrated PL intensity as a function of temperature for $CsPbCl_3:Mn^{2+}$ sample.

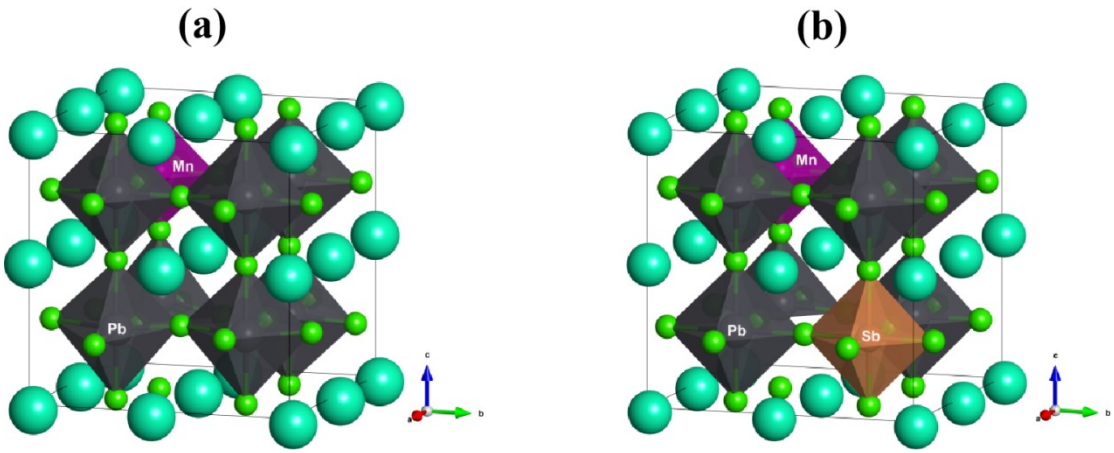

Fig. S6. The optimized structure of (a) $CsPbCl_3:Mn^{2+}$ and (b) $CsPbCl_3:Mn^{2+}$, Sb^{3+} structures.

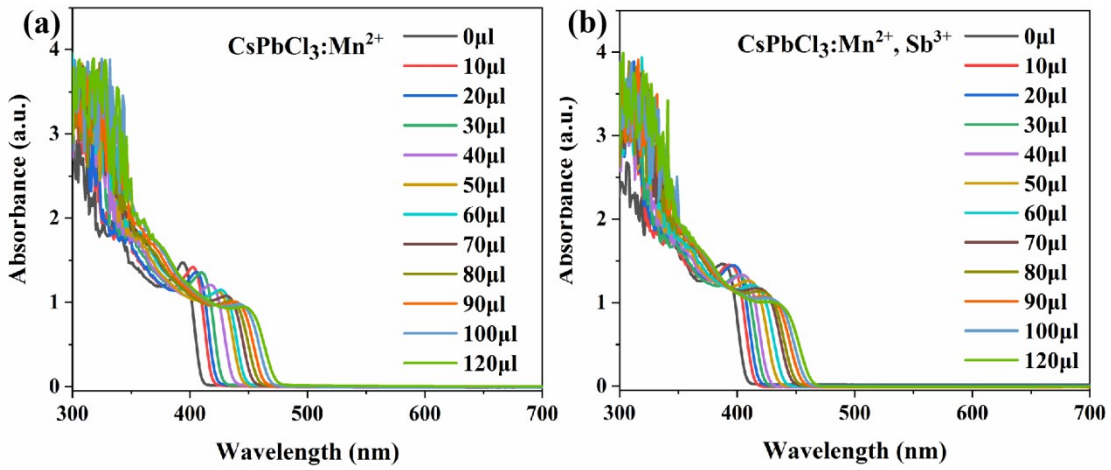

Fig. S7. Absorption spectra of (a) $CsPbCl_3:Mn^{2+}$ and (b) $CsPbCl_3:Mn^{2+}$, Sb^{3+} samples after anion exchange with varying amounts of $PbBr_2$.

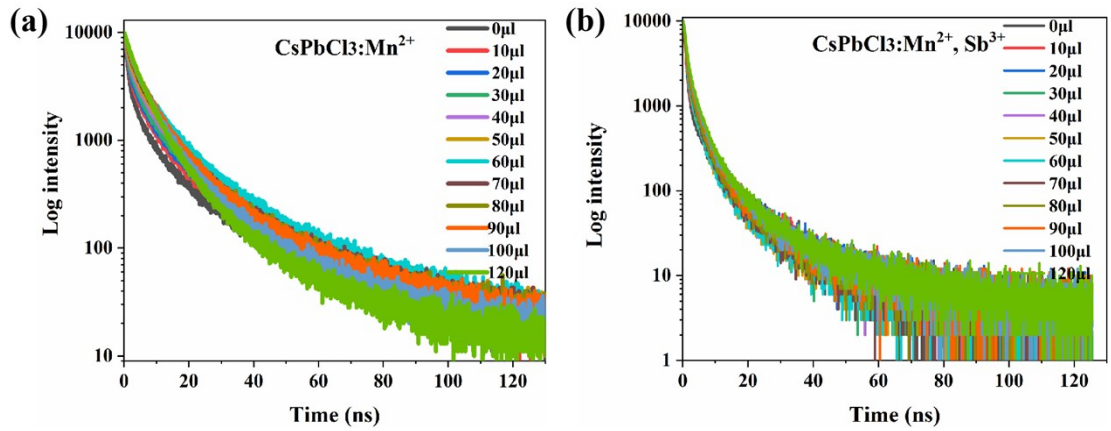

Fig. S8. Time-resolved PL spectra of exciton emission for (a) $CsPbCl_3:Mn^{2+}$ and (b) $CsPbCl_3:Mn^{2+}$, Sb^{3+} samples.

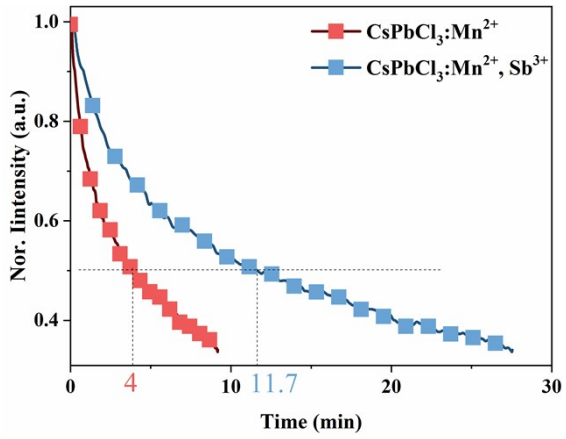

Fig. S9. Device stability for $CsPbCl_3:Mn^{2+}$ (red) and $CsPbCl_3:Mn^{2+}$, Sb^{3+} (blue) samples.

Table S1. Average lifetime data of Mn^{2+} after single exponential fit for $CsPbCl_3$ NCs with different feed moral ratio of Mn^{2+}/Sb^{3+}.

Mn/Sb	**0.3/0**	**0.5/0**	**0.1/0.5**	**0.3/0.5**	**0.5/0.5**
T_{ave}**/ms**	1.63	1.73	1.70	1.68	1.67

Table S2. Emission decay of exciton for $CsPbCl_3$ NCs with different moral ratios of Mn^{2+}/Sb^{3+}.

Mn^{2+}/Sb^{3+}	0.1/0	0.3/0	0.5/0	0.1/0.5	0.3/0.5	0.5/0.5
A1	9028.43	8526.48	8722.90	9064.97	9773.19	11054.68
T_1/ns	1.38	1.31	1.21	1.07	0.95	0.99
A2	1511.07	2067.68	1987.23	1648.21	1001.16	533.07
T_2/ns	16.0	10.39	8.04	8.15	5.37	4.41
T_{ave}/ns	10.96	10.39	8.04	8.15	5.37	4.41

Table S3. Summary of the performance of Violet LEDs.

Emission layer materials	EL peak position (nm)	Max EQE (%)	Luminance (cd/m^2)	Ref
$Cs_3Sb_2Br_9$ QDs	408	0.21	29.60	37
Cs_3CeBr_6 crystal	391	0.46	-	38
$CsPbCl_3$:Mg NCs	402	0.1	135	39
$CsPbCl_3$:Mn^{2+}, Sb^{3+} NCs	413	0.39	121	**This work**

References:

1. Kresse. G.; Furthmuller. Efficiency of ab-initio total energy calculations for metals and semiconductors using a plane-wave basis set. *J. Comput. Mater. Sci.*, 1996, **6**, 15–50.

2. Perdew. J. P.; Burke. K.; Ernzerhof. M. Generalized Gradient Approximation Made Simple. *Phys. Rev. Lett*., 1996, **77**, 3865–3868.